Journal of Applied Polymer Science

Efficacy of La^{3+} entrapped chitosan bio-polymeric matrix for the recovery of oil from oil-in-water emulsion

S. SD. Elanchezhiyan, N. Sivasurian, Sankaran Meenakshi
Department of Chemistry, The Gandhigram Rural Institute-Deemed University, Gandhigram 624 302, Tamil Nadu, India
Correspondence to: S. Meenakshi (E-mail: drsmeenakshi@gmail.com)

ABSTRACT: On the basis of the present study, the details of the recovery of cutting oil from oil-in-water emulsion using the modified forms of biopolymer chitosan viz., chitosan beads (CB), carboxylated chitosan beads (CCB), and lanthanum incorporated carboxylated chitosan beads (La-CCB). Various oil sorption experiments were conducted using an extractive gravimetric method by optimizing various parameters such as contact time, pH, sorbent dosage, and initial oil concentration for maximum sorption. It was found that the oil removal percentage was comparatively less in the case of CB and CCB when compared with La-CCB, which showed 85% of oil removal at acidic condition. The obtained adsorption equilibrium data was explained with Freundlich, Langmuir, D–R, and Tempkin isotherms to find the best fit for the sorption process. Thermodynamic parameters such as ΔG^0, ΔH^0, and ΔS^0 were calculated in order to understand the nature of sorption process. The surface morphology and sorption of oil on the beads were confirmed by FTIR, SEM with EDAX, XRD, TGA, and DSC analysis. This work provides a potential platform for the expansion of oil removal technology. © 2015 Wiley Periodicals, Inc. J. Appl. Polym. Sci. **2016**, *133*, 43218.

KEYWORDS: adsorption; chitosan; emulsion; oil

Received 31 July 2015; accepted 9 November 2015
DOI: 10.1002/app.43218

INTRODUCTION

In the present scenario, the threat of oil pollution has become a major environmental concern with the increasing oil exploration and production activities. Owing to industrial growth globally, annual worldwide usage of petroleum-based products and vegetable oils are increasing and is estimated to surpass 100 and 92 million tonnes, respectively.[1] Not all countries have set maximum allowable limit for oil and grease in water, unlike other water pollutants. For instance, the maximum limit for oil and grease in drinking water is not stated in World Health Organization (WHO)[2]; but the United States Environmental Protection Agency (USEPA) limits oil and grease content in drinking water to 0.3 mg/L.[3] The Ministry of Environment and Forests, Government of India has prescribed the discharge wastewater quality with oil concentration not exceeding 5 mg/L.[4] When oil meets water, it forms emulsion, which needs to be treated before it is disposed.[5–8] The majority of the industrial wastewaters contain oil-in-water emulsions as basic contaminates which generates serious ecological problem to the environment owing to the toxic and hazardous properties of its components.[9,10] Cutting fluid consist of a suspension of oil droplets in water stabilized by surfactants, and usually contain several compounds such as biocides, defoamers, rust inhibitors, coupling agent, extreme pressure additives, etc.[11] As a result, cutting fluid has to be replaced after use, and at last, a significant amount of cutting fluid is commonly found in wastewater. Improper disposal of the cutting fluid containing waste from metal manufacturing plants creates environmental crisis.[12] Long-term exposure to the metalworking fluids can lead to the augmented prevalence of several types of cancer. The international agencies for research on cancer have proved that mineral oils used in the workplace are carcinogenic in nature.[13] Therefore, it is necessary to remove cutting fluid from industrial wastewater before discharging them into the environment.

Several techniques have been proposed by researchers to recover oil from wastewater and these have merits as well as demerits. The techniques are adsorption,[14–23] flocculation,[24] coagulation,[25–27] electro-coagulation,[28] flotation,[29–31] membrane technique,[32–35] biological treatment,[36,37] etc. Existing methods for the treatment of oily wastewater before their disposal remain unsatisfactory because of their expensive or incomplete process. Among all the methods, adsorption is an environmental friendly and low cost method that requires simple technology and is becoming the method of choice. Different materials have been proposed for the treatment of oil adsorption such as chitosan,[15–18,21,25] walnut shell,[38] sawdust,[7,11,26] vermiculite,[14] barley straw,[16] coal,[17] corn straw,[19] activated carbon,[39] mixture of Ca and Mg oxides,[40] raw cotton,[41] organoclay,[42] etc., and they have

Table I. Properties of Cutting Oil Selected for This Present Work

S. No.	Characteristics	Method	Specification
1	Appearance @ 30°C	Visual	Clear liquid
2	Density @ 29.5°C, g/mL	IS 1115-86 P: 32	0.869
3	Water content, % wt	IS 1115-86 P: 40	1.6
4	Flash point, (COC), °C	IS 1115-86 P: 69	176
5	Kinematic viscosity @ 40°C, cSt.	IS 1115-86 P: 25	24.1
6	Particle size of 4% cutting oil Emulsion, mμ	CILAS 930 particle size analyzer	1.66
7	Zeta potential value, mV	Malvern Zeta Seizer	−90.9

been investigated for the removal of oil. Among these chitosan is a natural polysaccharide, eco-friendly and one of the effective, acceptable biosorbent commonly used in wastewater system owing to its outstanding properties such as biocompatibility, biodegradability, hydrophilicity, adsorption property, and antibacterial property.[21] The flexible structure in the polymeric chain of chitosan enables it to adopt the suitable configuration for complexation with metal ions.[43] Oil removal using chitosan bead (CB) was found to be negligible, which implies that the reactive amino and hydroxyl groups were not involved in oil sorption. To effectively make use of both the hydroxyl and amino groups present in chitosan, carboxylation followed by chelating of amino groups using La^{3+} was carried out. Consequently, the ultimate goal of the present work is to study the effect of La^{3+} incorporation in chitosan beads by chelating with the amine groups of chitosan in which the —OH group has been already converted to —COOH form (CCB), as the oil sorption using unmodified chitosan was negligible. The oil sorption using CB, CCB, and metal entrapped CCB (La-CCB) have been compared and the enhancement of oil sorption using the La-CCB has been explained.

In the present work, La^{3+} entrapped carboxylated chitosan beads (La-CCB) were used for the removal of cutting fluid from oil-in-water emulsion and the influence of different parameters, such as contact time, pH, sorbent dosage and initial concentration of cutting fluid on the sorption of oil were optimized. The isotherm models have been used to explain the experimental data of the oil sorption. This information would be useful for further application in removal of cutting fluid effluents particularly in metal working industries.

MATERIALS AND METHODS

Experimental Materials

Synthetic cutting fluid in oil-in-water emulsion form was obtained commercially which has been diluted into required concentration and used as oily wastewater. The properties of cutting oil are given in Table I. Chitosan flakes (85% deacetylated) was acquired from Pelican Biotech and Chemicals Labs, Kerala (India) and used without any further purification. The following analytical grade chemicals were used in the experimental work: n-hexane (Merck, Mumbai), $LaCl_3 \cdot 7H_2O$ (Sigma Aldrich, Mumbai), HCl, NaOH, glacial CH_3COOH, glutaraldehyde, and chloroacetic acid (CDH, New Delhi). Double distilled water was used throughout the experiment.

Preparation of La^{3+} Incorporated Carboxylated Chitosan Beads (La-CCB)

Cross-linked chitosan beads (CB) were prepared and used glutaraldehyde (2.5%) as a cross-linker to increase its stability as

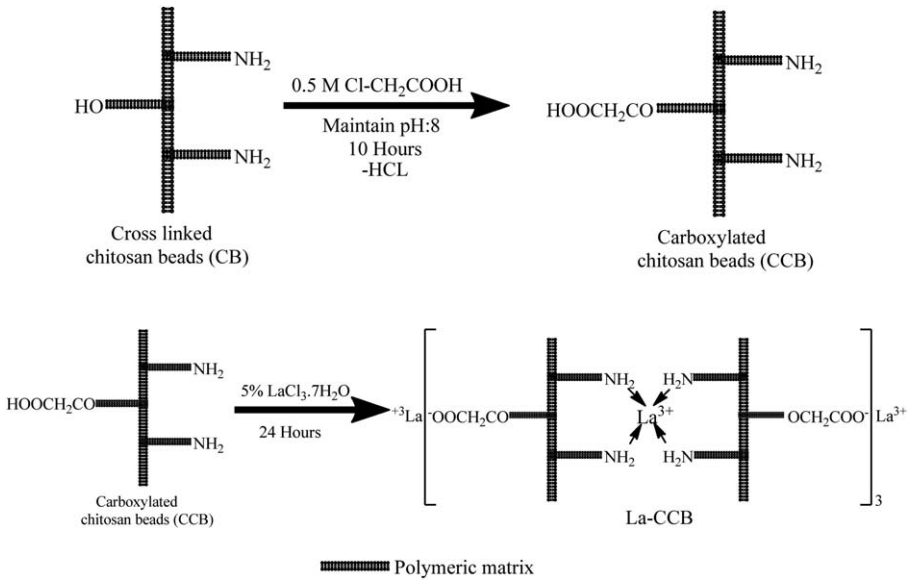

Scheme 1. Preparation of La-CCB.

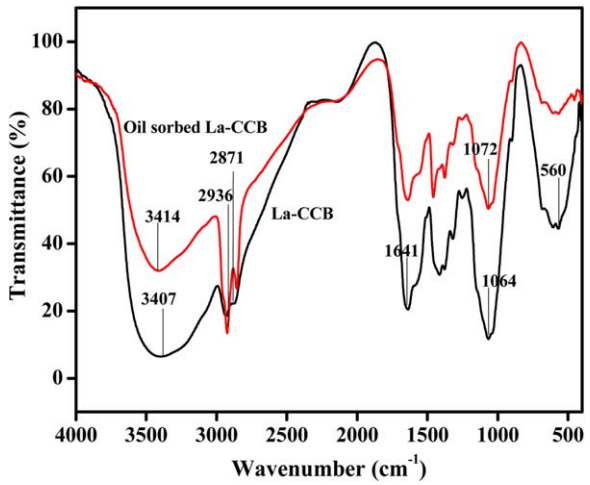

Figure 1. FTIR spectra of La-CCB and oil sorbed La-CCB. [Color figure can be viewed in the online issue, which is available at wileyonlinelibrary.com.]

reported in the earlier literature by Jeon and Holl.[44,45] The wet CB was carboxylated by 0.5*M* chloroacetic acid maintained at pH 8.0 using 0.1*M* NaOH for ten hours at ambient temperature to convert hydroxyl groups of chitosan to carboxyl groups. Then, the carboxylated chitosan beads (CCB) were washed with double distilled water to attain the neutral pH and allowed to dry at room temperature. The amine groups present in CCB were chelated with La^{3+} by treating CCB with 5% $LaCl_3 \cdot 7H_2O$ solution for 24 h, washed with double distilled water to attain a neutral pH and dried at room temperature[45] and is shown in Scheme 1.

Sorption Experiments

The sorption experiments were carried out by series of batch equilibration method in duplicate under similar conditions. Before sorption, the pH of the emulsion was adjusted to the desired value by adding respective 0.1*M* HCl or 0.1*M* NaOH. Adsorption experiments were performed by adding 400 mg of sorbent in a 25 mL of 4% oil-in-water emulsion of initial concentration prepared by dissolving 40 g cutting oil in 1000 mL distilled water. The mixture was shaken thoroughly at a speed of 180 rpm and at ambient temperature to reach equilibrium. At various time intervals, the mixture was taken to find out the residual concentration of the oil-in-water emulsion. The isotherm and thermodynamic parameters of sorption were

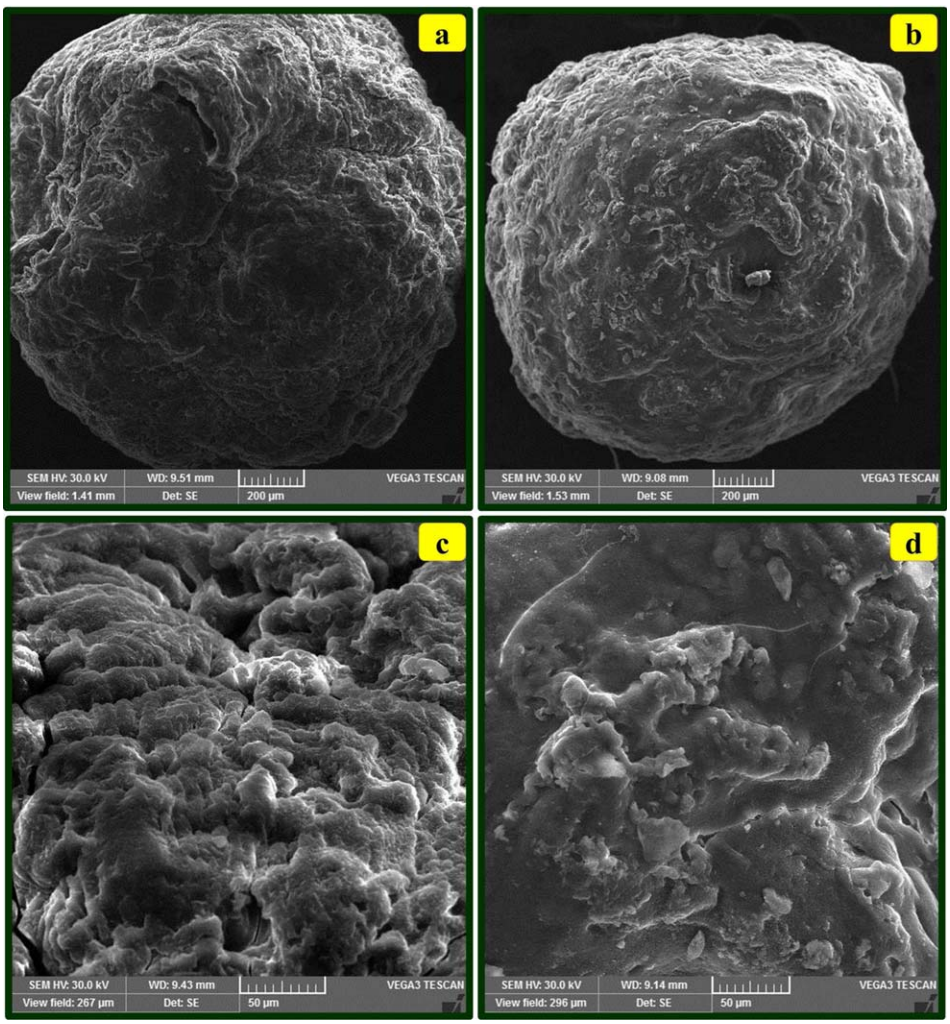

Figure 2. SEM images of (a) overall shape of La-CCB; (b) overall shaped of oil sorbed La-CCB; (c) La-CCB; and (d) oil sorbed La-CCB. [Color figure can be viewed in the online issue, which is available at wileyonlinelibrary.com.]

established by conducting the experiments at different initial oil concentrations viz., 3%, 4%, 5%, and 6% at 303 K, 313 K, and 323 K in a thermally controlled mechanical shaker. The percentage of oil removal using prepared sorbents was studied by optimizing various parameters such as contact time, pH, dose, and initial concentration of oil-in-water emulsion. The final concentration of the residual oil in each sample mixture was determined using n-Hexane as the oil-extraction solvent in accordance with the APHA standard recommended method for examining water and wastewater.[46] Then the solution was filtered at the appropriate time and the residual oil concentration was measured.

The oil removal percentage was calculated by the following equation,

$$\text{Oil removal } (\%) = \frac{C_i - C_e}{C_i} \times 100 \quad (1)$$

where C_i and C_e are the initial and equilibrium concentration of the oil-in-water emulsion.

Characterization of the Sorbent

Fourier Transform Infrared (FTIR) spectra of the La-CCB and the oil sorbed La-CCB were used to confirm the functional groups present in the sorbent within the wavelength range of 400–4000 cm^{-1} using JASCO-460 plus model. The surface morphology of the La-CCB before and after sorption were examined by scanning electron microscope (SEM) with VEGA3TESCAN model and the elemental analysis was made by energy dispersive analysis of X-ray (EDAX) spectroscopy with Bruker Nano Gmbh, Germany. XRD was applied to determine the crystalline phases of the La-CCB and oil sorbed La-CCB using XRD, X'per PRO model–PANalytical make. Thermal stability of the beads was determined by Thermo gravimetric analysis (TGA, Model 2960, Universal V2.4F TA instruments, The United States) and Differential Scanning Calorimetry (DSC, Model 2920, Universal V2. 4F TA Instruments, The United States). The water contact angle of the sorbents was measured on a drop shape analysis instrument (KRUSS DSA 4, Germany) with deionized water at ambient temperature. Heat of combustion of sorbents was measured by Model Parr 6200 Calorimeter (Parr Instruments Company, The United States). The pH at the potential of zero charge of the sorbents was measured using the pH drift method. The pH measurements of the emulsion were done using expandable ion analyzer EA940 with the pH electrode.

Statistical Tools

Computations were made using Microcal Origin (Version 8.0) software. The significance of data and goodness of fit was discussed using regression correlation coefficient (r).

RESULTS AND DISCUSSION

Characterization of La-CCB

The FTIR analysis was carried to find out the functional groups present in the as-synthesized La-CCB and oil sorbed La-CCB as it could be seen in Figure 1. The FTIR spetrum of La-CCB, a broad and strong absorption bands at 3407 cm^{-1} and 3414 cm^{-1} due to —OH and —NH_2 stretching vibrations of La-CCB and oil sorbed La-CCB respectively clearly indicates the presence of —OH and —NH_2 group present in the chitosan polymeric matrix. The

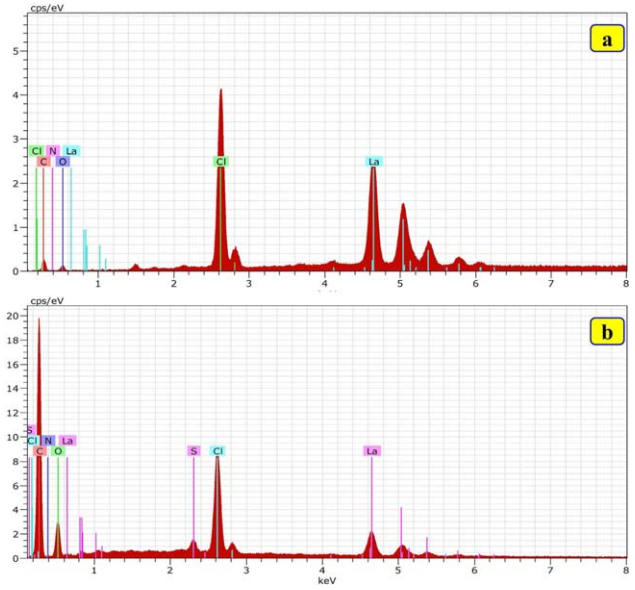

Figure 3. EDAX spectra of (a) La-CCB and (b) oil sorbed La-CCB. [Color figure can be viewed in the online issue, which is available at wileyonlinelibrary.com.]

above-mentioned bands are corresponds to —NH_2 stretching vibration of the amino group, even though, there is a possibility of overlapping between the —NH_2 and —OH stretching vibrations. In La-CCB, the two main characteristic bands at 2936 and 2871 cm^{-1} were revealed as asymmetric and symmetric stretching vibration of alkyl groups present in the chitosan matrix.[16] A wavenumber at 1641 cm^{-1} was assigned for —NH_2 bending vibration of chitosan moiety in La-CCB. The C-O stretching vibrations were noticed at 1064 and 1072 cm^{-1} of La-CCB and oil sorbed La-CCB respectively. A band at 560 cm^{-1} was corresponding to lanthanum present in the chitosan polymeric matrix (—La—N vibrations and La—O vibrations). After oil sorption, the peaks at 2936 and 2871 cm^{-1} were increased due to the alkyl group present in the cutting oil.[21] The notable peak shift from 1064 to 1072 cm^{-1} was owing to the interaction between —OH groups of chitosan with the La^{3+} ions. Moreover, the significant shifting of majority of the peaks to lower wavenumber in the oil sorbed La-CCB, which may be taken as an indication of oil sorption onto La-CCB.

Investigations were made on the surface morphology of La-CCB and oil sorbed La-CCB and are shown in Figure 2. Overall image of La-CCB and oil-sorbed La-CCB are shown in Figure 2(a,b). La-CCB reveals rough and uneven surface and shown in Figure 2(c). The uneven surface of La-CCB was completely destroyed owing to the oily layer formed on La-CCB which is shown in Figure 2(d). Figure 2(d) confirms a significant change in the structure of the sorbent, which is an evidence of the oil sorption.

The EDAX spectra of the La-CCB and oil sorbed La-CCB are represented in Figure 3(a,b), which confirm the presence of C, N, O, and La. The elemental analyses provided a direct confirmation that the lanthanum was successfully entrapped on the surface of the chitosan polymeric matrix. In addition, the oil

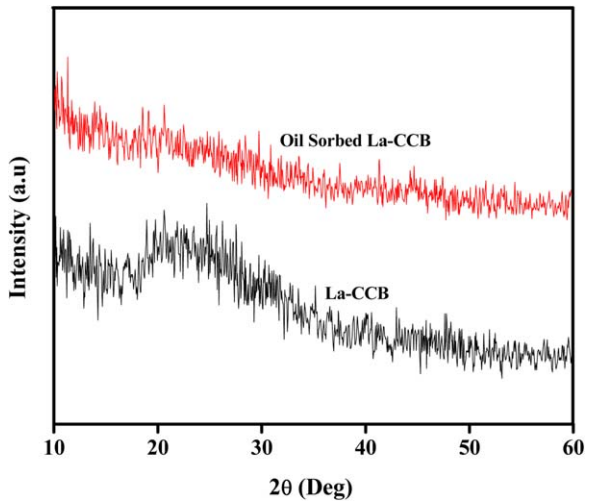

Figure 4. XRD pattern of La-CCB and oil sorbed La-CCB. [Color figure can be viewed in the online issue, which is available at wileyonlinelibrary.com.]

sorption occurred onto La-CCB was confirmed by the higher percentage of carbon and presence of the sulfur peak as the oil has both carbon and sulfur.

The XRD pattern of La-CCB and oil sorbed La-CCB are shown in Figure 4. The XRD spectrum of La-CCB has 2θ diffraction peak at 20° and other peaks with much weaker intensity. This peak corresponds to a crystalline structure of a chitosan polymeric matrix.[47] The oil sorbed La-CCB shows the peak at 44.66° and this shift after oil sorption resulted in the significant decrease in the crystallinity of oil sorbed La-CCB, which suggests a slight change in the surface morphology of the oil sorbed La-CCB. The less crystalline nature of oil sorbed La-CCB indicates that the percentage of the disordered regions on the sorbent surface increased, which was advantageous for oil sorption and storage.[19]

In order to assess the thermal properties of La-CCB, TGA, and DSC analysis were performed, and are shown in Figure 5. There are two stages of degradation in the TGA curve of La-CCB, which is depicted in Figure 5(a). The first stage starts from 50°C and continues up to 200°C. It is to be noticed that there was about 12% weight loss due to the loss of adsorbed and bound water, which could not be removed completely by drying. Maximum weight loss occurs in the temperature range of 200°C–450°C and no significant thermal event occurs after 450°C. Around 83.9% of La-CCB is disintegrated within 800°C. At the end of the experiment, that is, at 800°C, only 11.47 mg of La-CCB remains as residue. Generally, chitosan cross-linked with glutaraldehyde had more thermal stability when compared with chitosan as reported by Acharyulu *et al.*[48] Thus, La-CCB possesses higher thermal stability.

In the DSC curve of La-CCB, the observed endothermic peak around 85°C could be attributed to the moisture present in the beads, which is shown in Figure 5(b). Generally, the DSC of cross-linked chitosan beads did not show any sharp exothermic peak.[48] But in the case of La-CCB, a sharp exothermic peak at 275°C may be due to the modification of cross-linked chitosan bead by carboxylation and incorporation of metal into it.

Figure 6 shows the contact angle images of CB and La-CCB. The contact angle of chitosan bead was found to be 81.7° [Figure 6(a)] and La-CCB [Figure 6(b)] shows 90.5° with deionized water. The chitosan polymeric matrix has primary amine groups, which shows the less hydrophobic property of chitosan. Therefore, metal loading on chitosan is a promising strategy for improving the hydrophobic properties, thus increasing the oil sorption capacity and selectivity in oil sorption from oil-in-water emulsion.

The calorific value of La-CCB and oil sorbed La-CCB were calculated using heat of combustion method. The calorific value of La-CCB was found to be 15,637 J/g but in the case of oil sorbed La-CCB it is enhanced to 18,640 J/g. This higher calorific value of oil sorbed La-CCB confirms the oil sorption onto La-CCB. After treatment, the oil sorbed sorbent can utilized as solid fuel.[21]

The net surface charge of the sorbent was estimated by pH zero point charge measurements (pHzpc).[49] The pHzpc of La-CCB was found to be 5.90, which clearly indicates that below this pH the surface is positively charged and above which La-CCB acquire a negative charge. At pH higher than pHzpc, the oil sorption is not favored.

Effect of Contact Time

The oil sorption of the sorbents viz., CB, CCB, and La-CCB were investigated by varying the contact time as a function in the range of 1–5 h. About 400 mg of each sorbent was added to 25 mL of 4% initial concentration of oil-in-water emulsion at

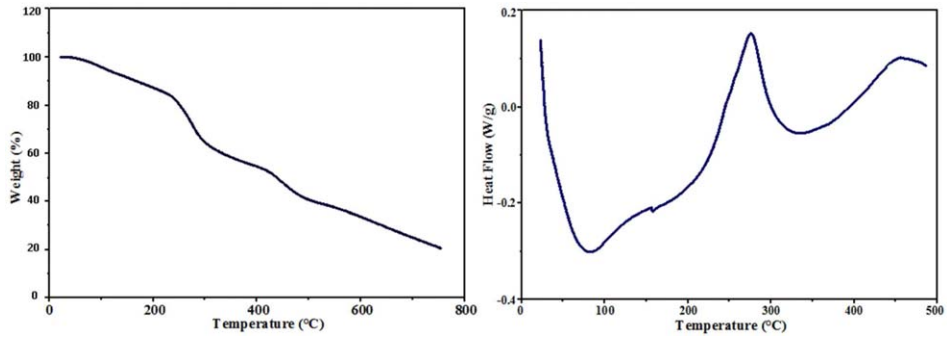

Figure 5. TGA of (a) La-CCB and DSC of (b) La-CCB. [Color figure can be viewed in the online issue, which is available at wileyonlinelibrary.com.]

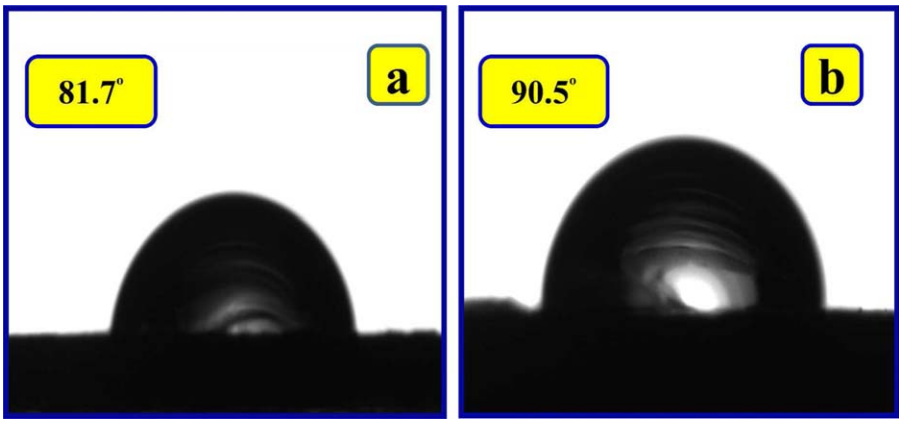

Figure 6. Contact angle images of (a) CB and (b) La-CCB. [Color figure can be viewed in the online issue, which is available at wileyonlinelibrary.com.]

pH 3.0 and were placed in a set of five iodine flasks of 250 mL capacity. The contents were shaken thoroughly using a thermo stated mechanical shaker at a speed of 180 rpm at ambient temperature, filtered, and analyzed. The maximum removal of cutting fluid was found to be 8% and 21% using CB and CCB respectively and is shown in Figure 7. However, in the case of La-CCB, the maximum removal of cutting fluid was found to be 85%. Since the percentage removal of cutting fluid was found to be negligible with CB and CCB, further studies were limited to La-CCB alone.

The effect of contact time for the oil adsorption on La-CCB is shown in Figure 7. La-CCB needs 4 h to adsorb the maximum quantity of oil from oil-in-water emulsion. Basically, the oil removal percentage was increased with the increasing interaction of oil and sorbent.[15] Contact time plays an important role at the beginning of adsorption process, due to the availability of sorbent surface and there is no significant change near equilibrium because of limited availability of sorbent surfaces for oil entrapment.[15,18] The adsorption of oil attained equilibrium at 4 h. The maximum removal of oil was found to be 85% using La-CCB as an adsorbent. Consequently, 4 h was fixed as the contact time for further experiments.

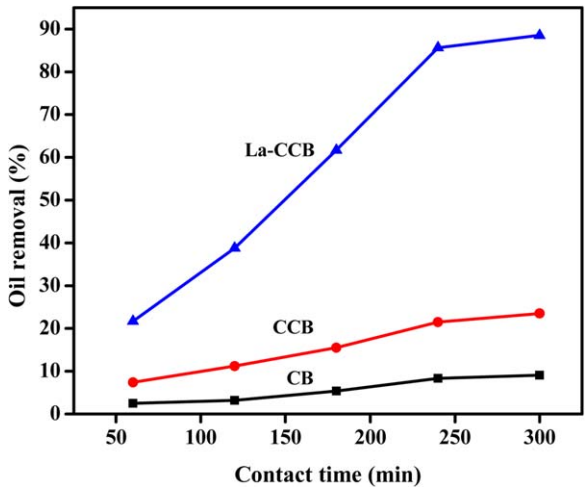

Figure 7. Effect of contact time on the removal of oil from oil-in-water emulsion using CB, CCB, and La-CCB in the presence of 4% initial oil concentration and 400 mg of sorbent dosage at pH 3. [Color figure can be viewed in the online issue, which is available at wileyonlinelibrary.com.]

Effect of pH

The adsorption of oil was very much dependent on the solution pH and it plays an eminent role in oil sorption studies. Figure 8 clearly indicates the effect of varying pH on the adsorption of oil using La-CCB. The maximum oil removal percentage was obtained at pH 3.0. The quantity of oil adsorbed by La-CCB was higher in acidic medium as compared with the basic medium and hence acidic medium acts as a catalyst.[21] The removal percentage of oil was decreased by increasing the pH of the emulsion. This may be due to the low degree of de-emulsification at the basic medium. Therefore, pH studies in the range of 3, 5, 7, 9, and 11 were also done to study the effect of adsorption of oil onto La-CCB. In strong acidic condition, La-CCB provokes a physico-chemical effect, apparently serving to demulsify and enhances the adsorption of oil. Hence, the acidic medium acts as a catalyst to adsorb oil molecules on sorbent. A significant change occurs at pH 3.0. Therefore,

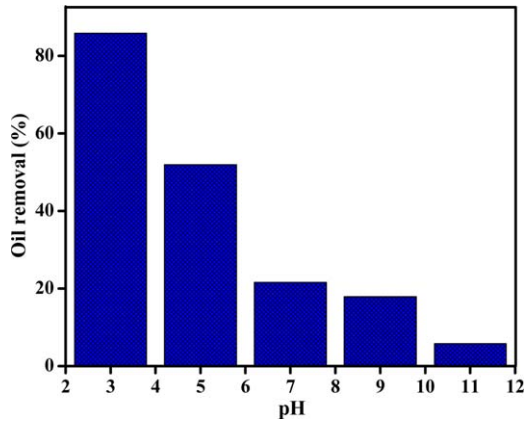

Figure 8. Influence of pH on the adsorption of oil from oil-in-water emulsion using La-CCB in the presence of 4% initial oil concentration and 400 mg of sorbent dosage with 4 h of contact time. [Color figure can be viewed in the online issue, which is available at wileyonlinelibrary.com.]

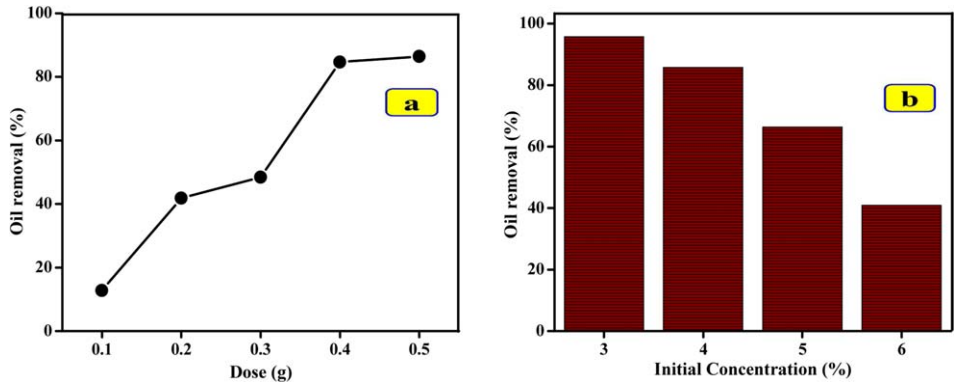

Figure 9. (a) Effect of dosage of La-CCB on the removal of oil from oil-in-water emulsion in the presence of 4% initial oil concentration with 4 h of contact time at pH 3 and (b) effect of initial oil concentration using La-CCB in the presence of 400 mg of sorbent dosage with 4 h of contact time at pH 3. [Color figure can be viewed in the online issue, which is available at wileyonlinelibrary.com.]

throughout the experiment, the pH of the emulsion was maintained at pH 3.0.

Effect of Adsorbent Dosage

The effect of different La-CCB dosages on cutting fluid removal was examined by varying the dose of La-CCB in the range from 100, 200, 300, 400, and 500 mg. In Figure 9(a), the percentage of oil removal increases with an increasing mass of adsorbent due to the increasing binding sites and surface sites.[15] So, the removal of oil was observed to be dependent on the dosage of La-CCB. The maximum oil removal percentage of 84% was attained with 400 mg of La-CCB by fixing the contact time as 4 h at pH 3.0. From this observation, 400 mg of sorbent dosage has been fixed as an optimum dosage for further studies.

Effect of Initial Oil Concentration

The effect of oil removal with various initial concentrations of oil was prepared in the range of 3%–6% at pH 3.0 using 400 mg of sorbent by fixing the contact time as 4 h. Figure 9(b) shows that the oil removal percentage decreases with increasing initial oil concentration. The decreasing percentage of oil removal can be explained by insufficient surface sites on sorbent, which would have become saturated above a certain oil concentration.

Sorption Isotherms

The interaction between the solid (sorbent) and the liquid phases (sorbate) at a range of concentrations are described by different sorption isotherm models at various temperatures. In the present study, the oil sorption capacity of La-CCB has been evaluated using commonly used adsorption isotherms namely Freundlich (1906), Langmuir (1916), Dubinin–Radushkevich (1947), and Tempkin (1940).

The linear form of Freundlich isotherm[50] is given in Table II. In this isotherm, q_e is the amount of oil adsorbed per unit weight of the La-CCB at equilibrium (mg/g), C_e is the equilibrium concentration of emulsion (mg/L), k_F is a measure of adsorption capacity, and $1/n$ is the adsorption intensity. The Freundlich isotherm constants k_F and n were determined from the slope and intercept of the plot, log q_e versus log C_e which is shown in Figure 10 and the values are presented in Table III. The values of $1/n$ are lying between 0.1 and 1.0, and the n value lying between 1 and 10 confirms the favorable conditions for adsorption.

Langmuir isotherm model[51] has four types and their linear forms are given in Table II. The Langmuir isotherm constants Q^0 and b are related to adsorption capacity and rate of adsorption respectively. The sorption capacity (Q^0) is the amount of adsorbate at complete monolayer coverage (mg/g) which gives the maximum sorption capacity of La-CCB. The values of Q^0

Table II. Isotherms and Their Linear Forms

Isotherms		Linear form	Plot
Freundlich	$q_e = k_F C_e^{1/n}$	$\log q_e = \log k_F + \frac{1}{n}\log C_e$	log q_e vs. log C_e
Langmuir Type-I	$q_e = \frac{Q^0 b C_e}{1+bC_e}$	$\frac{C_e}{q_e} = \frac{1}{Q^0 b} + \frac{C_e}{Q^0}$	$\frac{C_e}{q_e}$ vs. C_e
Langmuir Type-II		$\frac{1}{q_e} = \left[\frac{1}{Q^0 b}\right]\frac{1}{C_e} + \frac{1}{Q^0}$	$\frac{1}{q_e}$ vs. $\frac{1}{C_e}$
Langmuir Type-III		$q_e = Q^0 - \left[\frac{1}{b}\right]\left[\frac{q_e}{C_e}\right]$	q_e vs. $\frac{q_e}{C_e}$
Langmuir Type-IV		$\frac{q_e}{C_e} = bQ^0 - bq_e$	$\frac{q_e}{C_e}$ vs. q_e
Dubinin–Radushkevich	$q_e = X_m \exp(-k_{DR}\varepsilon^2)$	$\ln q_e = \ln X_m - k_{DR}\varepsilon^{DRDR2}$	ln q_e vs. ε^2
Tempkin	$q_e = \frac{RT}{b}\ln(K_T C_e)$	$q_e = B_T \ln K_T + B_T \ln C_e{}^e$	q_e vs. ln C_e

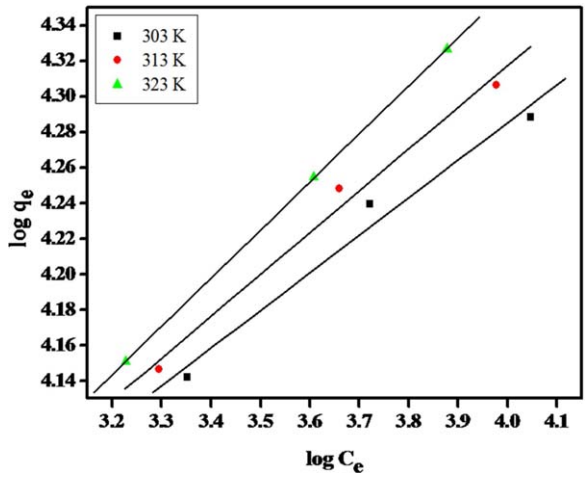

Figure 10. Freundlich isotherm for oil on La-CCB. [Color figure can be viewed in the online issue, which is available at wileyonlinelibrary.com.]

and b were determined from the respective slopes and intercepts of the straight line plots of four types of Langmuir isotherms viz., C_e/q_e versus C_e, $1/q_e$ versus $1/C_e$, q_e versus q_e/C_e, and q_e/C_e versus q_e as shown in Figure 11(a–d) and are shown in Table III. The Type-I Langmuir isotherm was found to be the best fit, as it has higher r value among the models studied.

The essential characteristics of the Langmuir isotherm can be expressed in terms of a dimensionless constant separation factor or equilibrium parameter, R_L[52]

$$R_L = \left(\frac{1}{1+bC_0}\right) \quad (2)$$

where b is the Langmuir isotherm constant and C_0 is the initial concentration of oil molecules (mg/L). The values of R_L were found to be less than 1 for oil adsorption onto La-CCB confirming that the adsorption process is favorable which is shown in Table III.

The linear form of D–R isotherm[53] model is given in Table II. X_m is the adsorption capacity (mg/g), k is the constant related to the adsorption energy (mol^2/J^2), and ε is the Polanyi potential which can be calculated using [eq. (3)]

$$\varepsilon = RT\ln\left(1+\frac{1}{C_e}\right) \quad (3)$$

Table III. Isotherm Parameters of La-CCB at Various Temperatures

		Temperature		
Isotherms	Parameters	303 K	313 K	323 K
Freundlich	$1/n$	0.2115	0.2350	0.2708
	n	4.7275	4.2553	3.6928
	$k_{F\ (mg/g)\ (L/mg)^{1/n}}$	2749.6030	2384.5696	1892.6922
	r	0.9882	0.9933	1.0000
Langmuir Type I	Q^0 (mg/kg)	21.2418	21.3287	21.3047
	b (L/g)	0.0009	0.0010	0.0012
	R_L	0.0248	0.0253	0.0271
	r	1.0000	0.9999	0.9987
Langmuir Type II	Q^0 (mg/kg)	21.2418	21.3287	21.3047
	b (L/g)	0.0009	0.0010	0.0012
	R_L	0.0224	0.0196	0.0169
	r	0.9707	0.9679	0.9639
Langmuir Type III	Q^0 (mg/kg)	21.5548	22.7403	24.1129
	b (L/g)	0.0008	0.0008	0.0008
	R_L	0.0244	0.0242	0.0237
	r	0.9997	0.9980	0.9822
Langmuir Type IV	Q^0 (mg/kg)	21.5572	22.7624	24.3439
	b (L/g)	0.0008	0.0008	0.0008
	R_L	0.0244	0.0243	0.0246
	r	0.9997	0.9980	0.9822
Dubnin-Radushkevich	k_{DR} (mol^2/J^2)	0.25855	0.20145	0.14934
	X_m (mg/kg)	19.0858	19.7828	20.4644
	E (kJ/mol)	1.3906	1.5754	1.8298
	r	0.9807	0.9738	0.9556
Temkin	k_T (L/g)	4.85E+03	1.07E+04	2.75E+04
	B_1	3481.8835	3973.8838	4700.5346
	r	0.9938	0.9977	0.9988

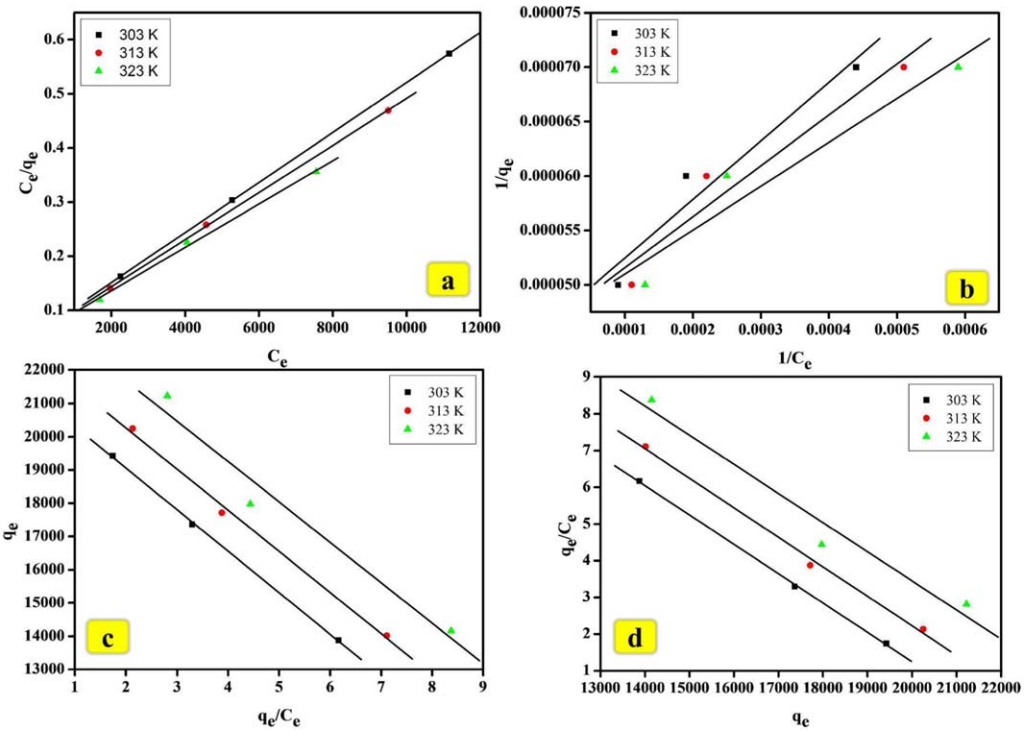

Figure 11. (a) Langmuir-I isotherm for oil on La-CCB. (b) Langmuir-II isotherm for oil on La-CCB. (c) Langmuir-III isotherm for oil on La-CCB. (d) Langmuir-IV isotherm for oil on La-CCB. [Color figure can be viewed in the online issue, which is available at wileyonlinelibrary.com.]

Figure 12 shows the plot of ln q_e versus ε^2 of the experimental data for the adsorption of oil molecules on La-CCB. The values of adsorption capacity, adsorption energy and Polanyi potential can be calculated from the slope and intercept. The isotherm parameters for the adsorption of oil molecules on La-CCB are shown in Table III.

The linear form of Tempkin isotherm model[54] is given in Table II. K_T is the equilibrium binding constant (L/g), and B_1 is related to the heat of adsorption, where $B_1 = RT/b$, T is the absolute temperature in Kelvin, and R is the universal gas constant, 8.314J/mol K. A plot of q_e versus ln C_e for the Tempkin isotherm yields a linear line, as shown in Figure 13. The adsorption data were analyzed according to the linear form of the Tempkin isotherm. The isotherm constants and regression coefficients are represented in Table III.

The corresponding regression coefficient values for all the isotherms are shown in Table III. From the r values, the best fit for the oil sorption on La-CCB among the various models studied is in the following order:

Langmuir-I > Langmuir-IV > Langmuir-III > Tempkin > Freundlich > D-R > Langmuir-II

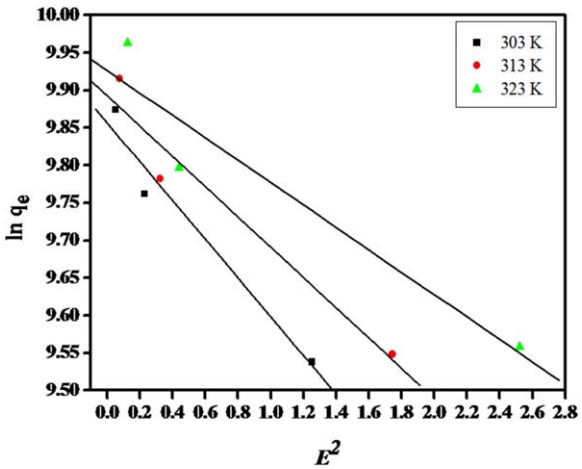

Figure 12. *D–R* isotherm for oil on La-CCB. [Color figure can be viewed in the online issue, which is available at wileyonlinelibrary.com.]

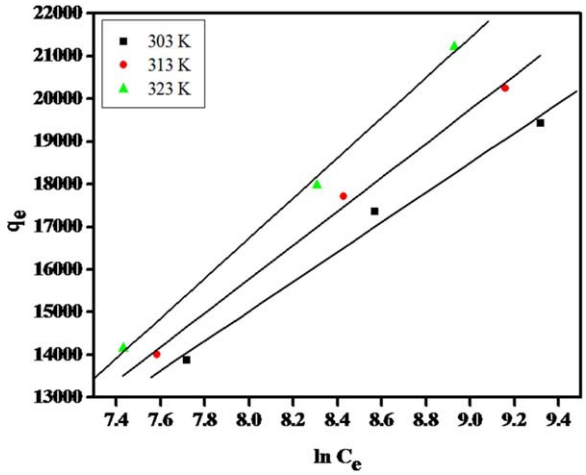

Figure 13. Tempkin isotherm for oil on La-CCB. [Color figure can be viewed in the online issue, which is available at wileyonlinelibrary.com.]

Table IV. Thermodynamic Parameters of La-CCB on the Oil Sorption

Thermodynamic parameters	Temperature	La-CCB
ΔG^0 (kJ/mol)	303 K	−22.40
	313 K	−22.83
	323 K	−23.13
ΔH^0 (kJ/mol)		11.41
ΔS^0 (kJ/K/mol)		0.04

From the above discussion, it is concluded that Langmuir-I was found to be more applicable for oil sorption compared with other isotherm models.

Thermodynamic Studies for the Sorption Process

Thermodynamic parameters of standard free energy change (ΔG^0), standard enthalpy change (ΔH^0), and standard entropy change (ΔS^0) were determined using the following equations:

$$\Delta G^0 = -RT\ln K_0 \quad (4)$$

$$\ln K_0 = \frac{\Delta S_0}{R} - \frac{\Delta H_0}{RT} \quad (5)$$

The free energy of sorption process, considering the sorption equilibrium coefficient K_0, is given in eq. (4) ΔG^0 is the standard free energy of sorption (kJ/mol), T is the temperature in Kelvin, and R is the universal gas constant (8.314 J/mol/K). The sorption distribution coefficient K_0, was determined from the slope of the plot $\ln(q_e/C_e)$ against C_e at different temperatures and extrapolating to zero C_e according to the method suggested by Khan and Singh.[55] ΔH^0 and ΔS^0 were calculated from the slope and intercept of van't Hoff plot of ln K_0 against $1/T$.

Table V. Removal of Various Toxic Ions Using Different Lanthanum Loaded Sorbents by Adsorption Method

S. No	Sorbent	Toxic ions removed	Reference
1	La(III)-loaded chelating resins/gels	Fluoride	57
2	La^{3+}-impregnated cross-linked gelatin	Fluoride	58
3	Lanthanum doped mesoporous SiO_2	Phosphate	59
4	Lanthanum incorporated chitosan	Fluoride	60
5	Lanthanum(III)-chelex resin	Phosphate	61
6	Lanthanum-loaded zeolite	Arsenic(V)	62
7	La(III) incorporated carboxylated chitosan beads	Fluoride	45
8	Lanthanum-modified bentonite	Phosphate	63
9	Lanthanum doped vesuvianite	Phosphate	64
10	Mixed lanthanum/aluminum pillared montmorillonite	Phosphate	65
11	Lanthanum hydroxide	Fluoride	66
12	Lanthanum(III) doped mesoporous silicates	Phosphate	67
13	La-incorporated chitosan beads	Fluoride	68
14	Lanthanum alginate bead	Fluoride	69
15	Orange waste loaded with multi-valent metal ions	Fluoride	70
16	Carbon fiber loaded with lanthanum oxide	Phosphate	71
17	Lanthanum(III)-coordinated diamino-functionalized 3D hybrid mesoporous silicates	Phosphate	72
18	Lanthanum impregnated chitosan flakes	Fluoride	73
19	Lanthanum(III) loaded granular ceramic	Phosphorus	74
20	La(III) encapsulated silica gel/chitosan composite	Chromium	75
21	Cu/Mg/Fe/La layered double hydroxide	Arsenate	76
22	Lanthanum loaded mesoporous MCM-41	Diesel fuel	77
23	Hydroxyl–iron–lanthanum doped activated carbon fiber	Phosphate	78
24	Aluminum and lanthanum modified natural materials	Fluoride	79
25	Lanthanum modified bentonite clay	Phosphate	80
26	Hybrid sorbent of zeolite/lanthanum hydroxide	Phosphate	81
27	La(III)-modified bentonite	Phosphate	82
28	Chitosan supported La-Zr-beads	Fluoride	83
29	Entrapped silica gel/chitosan biocomposite	Fluoride	84
30	La loaded silica chitosan composite	Phosphate	85
31	La^{3+} entrapped chitosan beads	Oil recovery	Present study

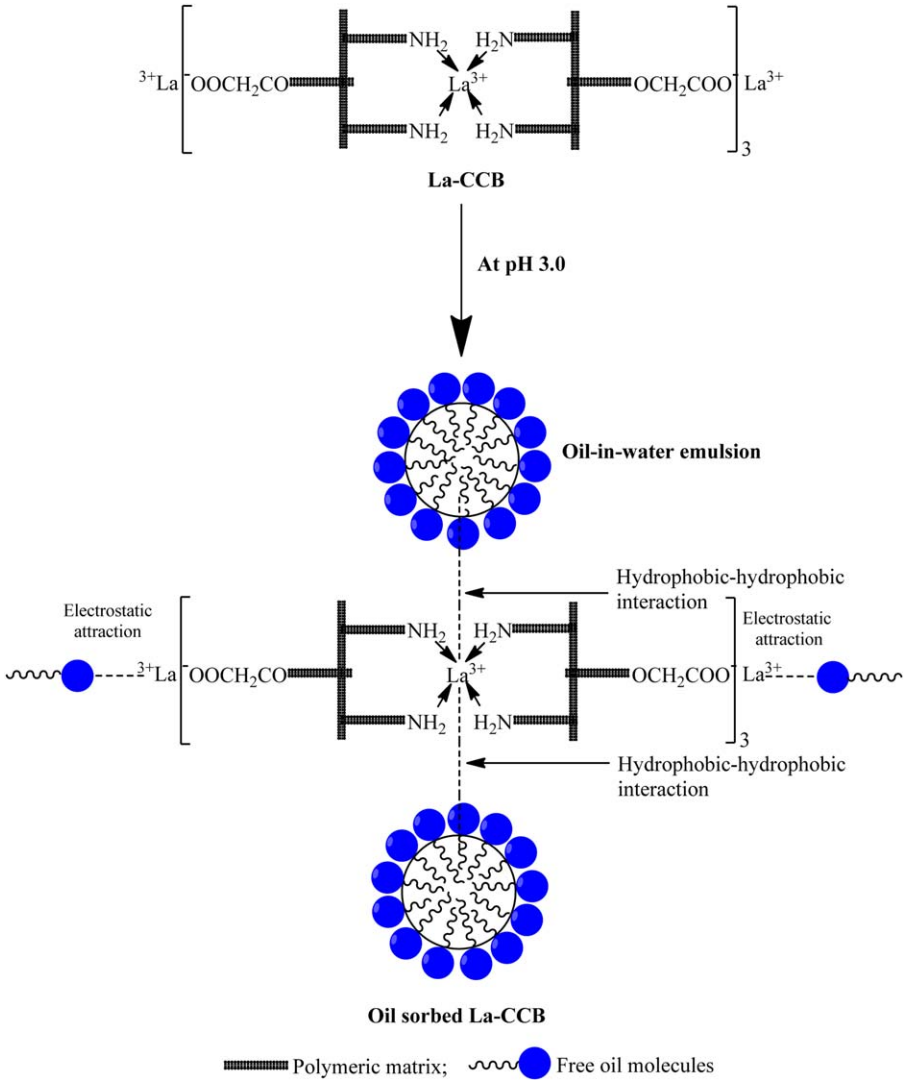

Scheme 2. Feasible mechanism of oil sorption using La-CCB. [Color figure can be viewed in the online issue, which is available at wileyonlinelibrary.com.]

The observed thermodynamic values for La-CCB were calculated and are shown in Table IV. The spontaneous nature of the oil sorption by La-CCB is confirmed by the negative values of ΔG^0. The positive value of ΔH^0 confirms the endothermic nature of the sorption process by La-CCB. The positive value of ΔS^0 indicates that the randomness increases at the solid-solution interface during oil sorption onto La-CCB.

Removal of Various Toxic Ions Using Lanthanum Entrapped Sorbents and Their Advantages

The utility of transition metals is well known in the field of water treatment; since it does not leach into water owing to its high positive character.[56] Lanthanum, in comparison with other transition metals exhibits more adsorption capability; it is non-toxic and environmentally friendly. Frequently, clays, chelating resins, mesoporous silica materials, activated carbon fibers, biopolymers like chitosan, etc., have been found to be a useful medium for loading/doping of lanthanum. A wide range of literature survey has been made regarding the removal of various toxic ions such as fluoride, phosphate, and a few heavy metals using lanthanum based sorbents[45,57–85] and is shown in Table V. But, while seeking literature regarding oil removal using lanthanum loaded sorbents, only a report on desulfurization of diesel fuel by lanthanum loaded mesoporous MCM-41 was found.[77] Hence, it was planned to study the removal of cutting fluid using La-CCB, as it has been seldom reported.

Oil Sorption Mechanism

The sorption of oil from the emulsion would take place after demulsification at acidic condition. Various types of attractive forces viz., chemical, electrostatic, and physical forces act together on the sorption of oil, and depending upon the situation, some forces act more significantly compared with the other forces.[86] However, the major force responsible for sorption is hydrophobic interaction between the sorbent and sorbate system, as the main constituent of cutting fluid is a hydrocarbon. The authors already reported that chitin showed higher efficiency than chitosan, as chitin is more hydrophobic owing

to the presence of acetyl groups.[87] In this case, when La^{3+} is entrapped with $-NH_2$ groups of chitosan, which inhibited the lone pair of electrons of nitrogen, which in turn enhanced the hydrophobic nature of chitosan and consequently La-CCB showed more sorption efficiency. Further, La^{3+} present in chitosan may also involve physical interaction with the oil part. The cutting fluid emulsion may also have emulsifiers and this may be electrostatically attracted along with the oil part by the charged end of the sorbent. Thus, all this force synergistically enhances the oil sorption efficiency of the sorbent. Further, FT-IR spectra and SEM micrographs confirms the adsorption performance of cutting fluid onto La-CCB. The mechanism of oil removal using La-CCB is shown in Scheme 2.

CONCLUSIONS

This work explores the adsorption of cutting fluid on La-CCB. The experimental result indicates that La-CCB was an effective sorbent to recover oil from oil-in-water emulsion. FTIR, SEM with EDAX, and XRD have elucidated the significant uptake of cutting fluid onto La-CCB by adsorption method. La-CCB shows the higher oil removal percentage at acidic condition with a contact time of 4 h for 4% initial oil concentration. pH plays an important role in oil sorption due to the higher degree of demulsification at acidic medium and the optimum pH for oil sorption was found to be pH 3.0. The adsorption of oil on La-CCB followed Langmuir-I isotherm model compared with other isotherm models discussed. The nature of oil sorption was spontaneous and endothermic which have been proved by thermodynamic parameters. The oil sorption mechanism using La-CCB follows the hydrophobic interaction through physical forces. The introduction of lanthanum on CCB enhanced hydrophobicity of CCB, which in turn adsorb the cutting fluid.

ACKNOWLEDGMENTS

The corresponding author is grateful to CSIR-MRP (23(0028)/14/EMR-II) New Delhi, India and the First author is thankful to UGC-BSR, New Delhi, India for providing financial support to carry out this research work.

REFERENCES

1. Abdullah, M. A.; Rahmah, A. U.; Man, Z. *J. Hazard. Mater.* **2010**, *177*, 683.
2. World Health Organization. Guidelines for Drinking-Water Quality, 4th ed., Geneva 27, Switzerland, **2011**.
3. Ahmad, A. L.; Chong, M. F.; Bhatia, S.; Ismail, S. *Desalination* **2006**, *191*, 35.
4. Ministry of Environment and Forests Notification, Environment (Protection) Amendment Rules, (Petroleum oil Refinery) G.S.R. India, **2008**.
5. He, G.; Chen, G. *Sep. Purif. Technol.* **2003**, *31*, 13.
6. Xia, L.; Lu, S.; Cao, G. *Sep. Sci. Technol.* **2003**, *38*, 4079.
7. Cambiella, A.; Ortea, E.; Rıos, G.; Benito, J. M.; Pazos, C.; Coca, J. *J. Hazard. Mater.* **2006**, *131*, 195.
8. Rajakovic, V.; Skala, D. *Sep. Purif. Technol.* **2006**, *49*, 192.
9. Quemeneur, M.; Marty, Y. *Water Res.* **1994**, *28*, 1217.
10. Srinivasan, A.; Viraraghavan, T. *J. Hazard. Mater.* **2010**, *175*, 695.
11. Cambiella, A. N.; Ortea, E.; Rios, G.; Benito, J. M.; Pazos, C.; Coca, J. *J. Hazard. Mater. B* **2006**, *131*, 195.
12. Sokovic, M.; Mijanovic, K. *J. Mater. Process. Technol.* **2001**, *109*, 181.
13. Raynor, P. C.; Cooper, S.; Leith, D. Evaporation of Polydisperse Multicomponent Oil Droplets, *Am. Ind. Hyg. Assoc. J.* **1996**, *57*, 1128.
14. Silva, U. G. D.; Melo, M. A. D. F.; Silva, A. F. D.; Farias, R. F. D. *J. Colloid Interface Sci.* **2003**, *260*, 302.
15. Ahmad, A. L.; Sumathi, S.; Hameed, B. H. *Water Res.* **2005**, *39*, 2483.
16. Ibrahim, S.; Wang, S; Ang, H. M. *Biochem. Eng. J.* **2009**, *100*, 5744.
17. Xiaobing, L.; Chunjuan, Z.; Jiongtian, L. *Mining Sci. Technol.* **2010**, *20*, 778.
18. Sokker, H. H.; El-Sawy, N. M.; Hassan, M. A.; El-Anadouli, B. E. *J. Hazard. Mater.* **2011**, *190*, 359.
19. Li, D.; Zhu, F. Z.; Li, J. Y.; Na, P.; Wang, N. *Ind. Eng. Chem. Res.* **2013**, *52*, 516.
20. Bera, A.; Kumar, T.; Ojha, K.; Mandal, A. *Appl. Surf. Sci.* **2013**, *284*, 87.
21. Piyamongkala, K.; Mekasut, L.; Pongstabodee, S. *Macromol. Res.* **2008**, *16*, 492.
22. Rajakovic, V.; Aleksic, G.; Radetic, M.; Rajakovic, L. *J. Hazard. Mater.* **2007**, *143*, 494.
23. Long, J. J.; Zu, Y. G.; Fu, Y. J.; Luo, M.; Mu, P. S.; Zhao, C. J.; Li, C. Y.; Wang, W.; Li, J. *RSC Adv.* **2012**, *2*, 5172.
24. Pinotti, A.; Bevilacqua, A.; Zaritzky, N. *Waste Manage.* **2001**, *21*, 535.
25. Ahmad, A. L.; Sumathi, S.; Hameed, B. H. *Chem. Eng. J.* **2006**, *118*, 99.
26. Fu, Y.; Chung, D. D. L. *Appl. Clay Sci.* **2011**, *53*, 634.
27. Inan, H.; Dimoglo, A.; Ims, S.; Ek, H.; Karpuzcu, M. *Sep. Purif. Technol.* **2004**, *36*, 23.
28. Tir, M.; Mostefa, N. M. *J. Hazard. Mater.* **2008**, *158*, 107.
29. Ramaswamy, B.; Kar, D. D.; De, S. *J. Environ. Manage.* **2007**, *85*, 150.
30. Moosai, R.; Dawe, R. A. *Sep. Purif. Technol.* **2003**, *33*, 303.
31. Mansour, L. B.; Chalbi, S. *J. Appl. Electrochem.* **2006**, *36*, 577.
32. Kocherginsky, N. M.; Tan, C. L.; Lu, W. F. *J. Membr. Sci.* **2003**, *220*, 117.
33. Li, L.; Ding, L.; Tu, Z.; Wan, Y.; Clausse, D.; Lanoiselle, J.-L. *J. Membr. Sci.* **2009**, *342*, 70.
34. Scott, K.; Jachuck, R. J.; Hall, D. *Sep. Purif. Technol.* **2001**, *22*, 431.
35. Moulai-Mostefa, N.; Brou, A.; Ding, L.; Joffrin, M. Y. *Mec. Ind.* **2005**, *6*, 203.
36. Walker, J. D.; Colwell, R. R.; Petrakis, L. *Appl. Microb.* **1975**, *30*, 79.
37. Pasila, A. *Mar. Pollut. Bull.* **2004**, *49*, 1006.

38. Srinivasan, A.; Viraraghavan, T. *Bioresour. Technol.* **2008**, *99*, 8217.
39. Inagaki, M.; Kawahara, A.; Nishi, Y.; Iwashita, N. *Carbon* **2002**, *40*, 1487.
40. Solisio, C.; Lodi, A.; Converti, A. B. M. D. *Water Res.* **2002**, *36*, 899.
41. Singh, V.; Kendall, R. J.; Hake, K.; Ramkumar, S. *Ind. Eng. Chem. Res.* **2013**, *52*, 6277.
42. Salehi, K.; Mowla, D.; Karimi, G. J. *Dispers. Sci. Technol.* **2012**, *33*, 1682.
43. Merrifield, J. D.; Davids, W. G.; MacRae, J. D.; Amirbahman, A. *Water Res.* **2004**, *38*, 3132.
44. Jeon, C.; Holl, W. H. *Water Res.* **2003**, *37*, 4770.
45. Viswanathan, N.; Meenakshi, S. *J. Colloid Interface Sci.* **2008**, *322*, 375.
46. APHA. Standard Methods for the Examination of Water and Wastewater, 21st ed., American Public Health Association, Washington, DC, **2005**.
47. Karthik, R.; Meenakshi, S. *Int. J. Biol. Macromol.* **2014**, *67*, 210.
48. Acharyulu, S. R.; Gomathi, T.; Sudha, P. N. *Der. Pharm. Lett.* **2013**, *5*, 354.
49. Ramon, M. V. L.; Stoeckli, F.; Castilla, C. M.; Marin, F. C. *Carbon* **1999**, *37*, 1215.
50. Freundlich, H. M. F. J. *Phys. Chem.* **1906**, *57A*, 385.
51. Langmuir, I. J. *Am. Chem. Soc.* **1916**, *38*, 2221.
52. Weber, W. J.; Morris, J. C. *J. Sanit. Eng. Div. Am. Soc. Civ. Eng.* **1964**, *90*, 79.
53. Dubinin, M. M.; Radushkevich, L. V. *Chem. Zentr.* **1947**, *1*, 875.
54. Tempkin, M. J.; Pyzhev, V. *Acta Physiochim. URSS* **1940**, *12*, 217.
55. Khan, A. A.; Singh, R. P. *Colloid Surf.* **1987**, *24*, 33.
56. Persy, V. P.; Behets, G. J.; Bervoets, A. R.; De Broe, M. E.; D'Haese, P. C. *Semin. Dial.* **2006**, *19*, 195.
57. Fang, L.; Ghimire, K. N.; Kuriyama, M.; Inoue, K.; Makino, K. J. *Chem. Technol. Biotechnol.* **2003**, *1047*, 1038.
58. Zhou, Y.; Yu, C.; Shan, Y. *Sep. Purif. Technol.* **2004**, *36*, 89.
59. Ou, E.; Zhou, J.; Mao, S.; Wang, J.; Xia, F.; Min, L. *Colloids Surf. A: Physicochem. Eng. Aspects* **2007**, *308*, 47.
60. Kamble, S. P.; Jagtap, S.; Labhsetwar, N. K.; Thakare, D.; Godfrey, S.; Devotta, S. *Chem. Eng. J.* **2007**, *129*, 173.
61. Wu, R. S. S.; Lam, K. H.; Lee, J. M. N.; Lau, T. C. *Chemosphere* **2007**, *69*, 289.
62. Hongping, P. U.; Jiangbo, H.; Zhe, J. *Acta Geol. Sin.* **2008**, *82*, 1015.
63. Haghseresht, F.; Wang, S.; Do, D. D. *Appl. Clay Sci.* **2009**, *46*, 369.
64. Li, H.; Ru, J.; Yin, W.; Liu, X.; Wang, J.; Zhang, W. *J. Hazard. Mater.* **2009**, *168*, 326.
65. Tian, S.; Jiang, P.; Ning, P.; Su, Y. *Chem. Eng. J.* **2009**, *151*, 141.
66. Na, C.; Park, H. *J. Hazard. Mater.* **2010**, *183*, 512.
67. Zhang, J.; Shen, Z.; Shan, W.; Chen, Z.; Mei, Z.; Lei, Y. *J. Environ. Sci.* **2010**, *22*, 507.
68. Thakre, D.; Jagtap, S.; Bansiwal, A.; Labhsetwar, N.; Rayalu, S. *J. Fluorine Chem.* **2010**, *131*, 373.
69. Yakun, H. U. O.; Wenming, D.; Xia, H.; Jingnian, X. U.; Chinese, J. *Chem. Eng.* **2011**, *19*, 365.
70. Paudyal, H.; Pangeni, B.; Inoue, K.; Kawakita, H.; Ohto, K.; Harada, H. *J. Hazard. Mater.* **2011**, *192*, 676.
71. Zhang, L.; Wan, L.; Chang, N.; Liu, J.; Duan, C.; Zhou, Q. *J. Hazard. Mater.* **2011**, *190*, 848.
72. Zhang, J.; Shen, Z.; Shan, W.; Mei, Z.; Wang, W. *J. Hazard. Mater.* **2011**, *186*, 76.
73. Jagtap, S.; Kumar, M.; Das, S.; Rayalu, S. *Desalination* **2011**, *273*, 267.
74. Chen, N.; Feng, C.; Zhang, Z.; Liu, R.; Gao, Y.; Li, M. *J. Taiwan Inst. Chem. Eng.* **2012**, *43*, 783.
75. Gandhi, M. R.; Meenakshi, S. *J. Hazard. Mater.* **2012**, *203–204*, 29.
76. Guo, Y.; Zhu, Z.; Qiu, Y.; Zhao, J. *J. Hazard. Mater.* **2012**, *239240*, 279.
77. Subhan, F.; Liu, B. S.; Zhang, Y.; Li, X. G. *Fuel Process. Technol.* **2012**, *97*, 71.
78. Liu, J.; Zhou, Q.; Chen, J.; Zhang, L.; Chang, N. *Chem. Eng. J.* **2013**, *216*, 859.
79. Sequeira, A. T.; Miranda, V. M.; Rios, M. S.; Hernandez, I. L. *J. Fluorine Chem.* **2013**, *148*, 6.
80. Reitzel, K.; Andersen, F.; Egemose, S.; Jensen, H. S. *Water Res.* **2013**, *47*, 2787.
81. Xie, J.; Wang, Z.; Fang, D.; Li, C.; Wu, D. *J. Colloid Interface Sci.* **2014**, *423*, 13.
82. Kuroki, V.; Bosco, G. E.; Fadini, P. S.; Mozeto, A. A.; Cestari, A. R.; Carvalho, W. A. *J. Hazard. Mater.* **2014**, *274*, 124.
83. Prabhu, S. M.; Meenakshi, S. J. *Water Process Eng.* **2014**, *2*, 96.
84. Viswanathan, N.; Pandi, K.; Meehakshi, S. *Int. J. Biol. Macromol.* **2014**, *70*, 347.
85. Sowmya, A.; Meenakshi, S. *Environ. Prog.* **2015**, *34*, 146.
86. Wahi, R.; Chuah, L. A.; Yaw Choong, T. S.; Ngaini, Z.; Nourouzi, M. M. *Sep. Purif. Technol.* **2013**, *113*, 51.
87. Elanchezhiyan, S. SD.; Sivasurian, N.; Meenakshi, S. *Int. J. Biol. Macromol.* **2014**, *70*, 399.